JOURNAL OF MATERIALS SCIENCE 24 (1989) 2324–2330

Some thermodynamic and kinetic aspects of icosahedral phase nucleation in Al–Mn

LIVIO BATTEZZATI, CARLO ANTONIONE
Dipartimento di Chimica Inorganica, Chimica Fisica e Chimica dei Materiali, Università di Torino, Via P. Giuria 9, 10125 Torino, Italy

FRANCESCO MARINO
Dipartimento di Ingegneria, Università di Trento, Trento, Italy

The nucleation and growth rates for quasicrystals in Al–Mn are computed and compared with those of equilibrium intermetallic compounds, by means of a model based on the classical nucleation and growth theory. The driving force for nucleation is obtained from the available thermodynamic information for this system at high temperature. The extrapolation of the difference in free energy between the phases is performed, following a procedure earlier established for glass-forming system, using the heat of transformation of the quasicrystals and an estimate of its entropy of fusion. A reasonable thermodynamic description of the quasicrystalline phase is obtained. The roles of the difference in free energy between the phases, of the interfacial tension and of heterogeneous nucleation on the critical cooling rates for quasicrystal formation are discussed.

1. Introduction

The recent discovery of icosahedral phases in some Al–Mn alloys rapidly quenched from the melt has prompted extensive scientific curiosity about their preparation, structure and properties. Some facts are well established, e.g. the need for high cooling rates for the production of most icosahedral phases; the dendritic morphology of the quasicrystals which often coexist with a supersaturated fcc solid solution; the apparently random nucleation of the phase [1]. Some other points are still in debate, in particular, the atomic structure of the icosahedral phase is unsolved [2]. Also, no attempt has been made to date to describe the quasicrystalline phases in terms of free-energy composition diagrams and to calculate transformation curves for their overall nucleation and growth processes, together with those of the competing equilibrium phases. In this paper we propose a calculation of the nucleation and growth rates for the phases appearing in $Al_{86}Mn_{14}$ and $Al_{80}Mn_{20}$ alloys, based on the classical theory of nucleation and growth of crystals.

Inspection of the Al–Mn phase diagram which has been recently redetermined and critically reinterpreted [3], shows that many intermetallic compounds are involved in the solidification of aluminium-rich alloys (Fig. 1). For example, in equilibrium conditions the first solid to form from the liquid at the $Al_{86}Mn_{14}$ composition is the μ-phase at 1191 K, followed by the peritectic formation of Al_6Mn at 978 K. It is well established that in this case the phase competing with the formation of quasicrystals during rapid solidification is Al_6Mn [4–6]. Though this is expected because it has the same composition as the alloy, its peritectic formation occurs 200 K below the liquidus where both λ-Al_4Mn and μ should have a substantial driving force for nucleation. In $Al_{80}Mn_{20}$ a metastable decagonal phase (T phase) is competing. However, considering the metastable extrapolation of the Al_6Mn–liquid and Al_4Mn–liquid phase boundaries, congruent melting points close to each other were derived for Al_6Mn at 1113 K and for Al_4Mn at 1153 K [3]. At these temperatures the free energy of the compounds equals that of the liquid and a possibility for their nucleation exists just below these points. Under these circumstances it is easy to understand that the partitionless solidification of Al_6Mn from the undercooled liquid should be favoured with respect to the segregation of the liquid giving λ-Al_4Mn or μ. The solidification pattern in Al–Mn is therefore the result of the competition among various phases of similar free energy. The icosahedral phase must be inserted among these and, although a higher free energy should be expected for it, it should not be too different in stability from the equilibrium phases. An attempt to establish this hierarchy on both thermodynamic and kinetic grounds is performed in the following sections.

2. Kinetics of solidification

In studying the kinetics of quasicrystal formation we will benefit from our previous modelling of glass formation in metallic systems [7]. This is justified on various grounds. The $Al_{86}Mn_{14}$ alloy has been amorphized by irradiation and reversibly transformed to the quasicrystalline structure [8]. This shows that metallic glasses may exist in the Al–Mn system as a phase with a higher free energy than the icosahedral

0022–2461/89 $03.00 + .12

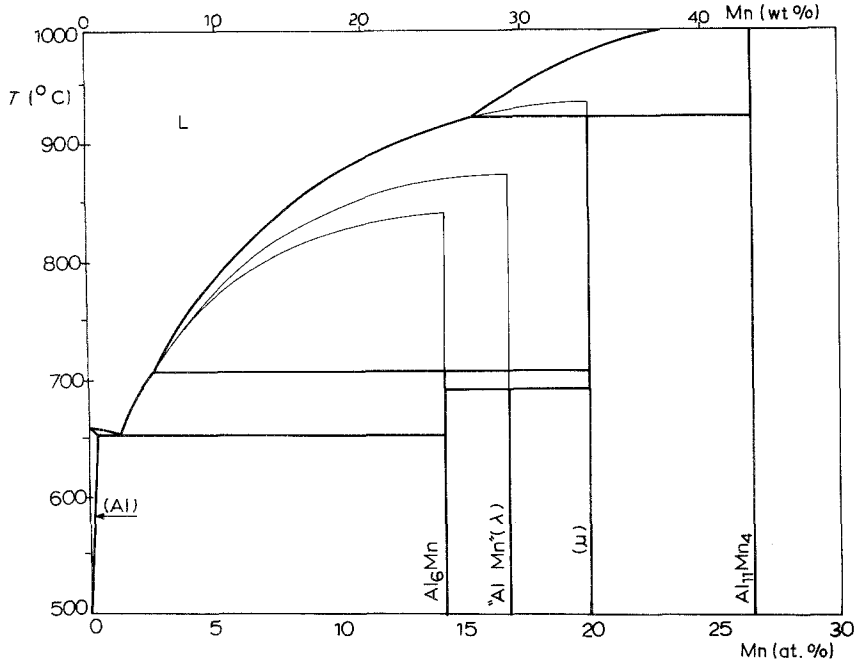

Figure 1 The aluminium-rich portion of the Al–Mn phase diagram (redrawn after Murray *et al.* [3]). Bold lines: equilibrium transformation curves; thin lines: computed metastable transformation curves for the intermetallic compounds.

(I) one. Moreover, the progressive substitution of aluminium with silicon, at first stabilizes the quasicrystalline phase in $Al_{75}Si_5Mn_{20}$, and then leads to the formation of amorphous alloys at the composition $Al_{64}Si_{16}Mn_{20}$ [9, 10]. The I-phase may be intermediate in stability between equilibrium and amorphous phases, even if no evidence has been found that the latter amorphous alloy transforms to the icosahedral phase, as happens for $Pd_{60}U_{20}Si_{20}$ [11]. The cooling rate necessary to obtain quasicrystals is of the same order as that necessary to obtain most metallic glasses, for which the suppression of equilibrium phase formation must also be accomplished. Therefore, we will compute by means of the nucleation and growth theory, the time necessary to produce a barely detectable fraction ($f \sim 10^{-6}$ in volume) of Al_6Mn at each temperature in order to assess its field of formation from the liquid in a TTT diagram. We will then show that a TTT curve for the icosahedral phase must be displaced to shorter times than the curve for compounds and discuss the parameters that determine its ease of formation.

In order to describe the formation of crystal phases from the liquid we must evaluate the quantities appearing in the equations for homogeneous nucleation, I_v, and growth rates, u_c, [12], respectively

$$I_v = \frac{DN_v}{a^2} \exp\left(-\frac{\Delta G^*}{kT}\right) \quad (1)$$

$$u_c = \frac{D}{a}\left[1 - \exp\left(\frac{\Delta G_m}{RT}\right)\right] \quad (2)$$

where D is the average diffusion coefficient in the liquid, N_v the mean atomic concentration for unit volume, a the mean atomic diameter. $\Delta G^* = 16\pi\gamma^3/3\Delta G_v^2$ is the driving force for nucleation of spherical particles, with γ the solid–liquid interfacial tension and ΔG_v the difference in free energy of liquid and crystalline phases per unit volume. In Equation 2 ΔG_m is the same quantity per mole. The case of heterogeneous nucleation of the equilibrium intermetallics will be briefly touched upon in the discussion.

The diffusion coefficient is usually related to the shear viscosity, η, through the Stokes–Einstein equation $D = kT/3\eta a_i$ where a_i is the ionic diameter. The viscosity of the Al–Mn liquid is not known, but the temperature dependence of viscosity for Al–Fe [13] and Al–Co [14] melts from which icosahedral phases have also been obtained by rapid quenching [10], parallels the case of glass-forming alloys. The data show rather high viscosity values, mainly at the equiatomic composition. Intermediate compositions follow this rise proportionally with respect to the values of the pure components. In addition, the viscosity deviates from an Arrhenian behaviour on approaching the liquidus, showing a more pronounced increase. So we assume that the viscosity of liquid Al–Mn at high temperature can be represented as in the similar Al–Fe and Al–Co systems at the corresponding temperature.

The viscosity in the undercooling regime is also likely to deviate from the Arrhenius behaviour and may be described by either Vogel–Fulcher–Tammann (VFT) or free volume (FV) equations [7]. In both cases a temperature should be defined at which atomic mobility is very low and viscosity tends to infinity. The glass transition temperature is used as this limit. The icosahedral phase in $Al_{86}Mn_{14}$ and $Al_{86}Fe_{14}$ transforms to the stable phases at about 700 K [15, 16]. This is also the temperature for the beginning of crystallization of $Al_{64}Si_{16}Mn_{20}$ [9, 10]. Therefore we will assume that the limiting temperature for atomic mobility in the liquid phase is around 700 K, i.e. the kinetic glass transition temperature at which viscosity is of the order of 10^{11} Pa sec [7]. The following equations are derived from the high-temperature experimental data and from the definition of T_g

$$\text{FV } \eta = 2.337 \times 10^{-4} \exp[0.04806 \exp(-9356.3/RT)] \quad (3)$$

$$\text{VFT } \eta = \exp[2106/(T - 658) - 10.404] \quad (4)$$

In Equation 4 $T_{g,0} = 658$ K is the ideal glass transition temperature. Both expressions represent the

property in a similar way [7] and the critical cooling rate for quasicrystal formation does not change very much if either Equation 3 or 4 are used. An Arrhenian extrapolation of the high-temperature viscosity down to 700 K should be ruled out because it would lead to such high nucleation and growth rates that the formation of the equilibrium Al–Mn compounds would occur under any quenching conditions. The results obtained using Equation 4 are reported below.

3. The difference in free energy of solid and liquid phases

The difference in free energy between the liquid and the solid has been computed in all cases in the undercooling regime from

$$\Delta G_m = \Delta H_m (T_m - T)/T_m - \int_T^{T_m} \Delta C_p \, dT + T \int_T^{T_m} \Delta C_p \, d \ln T \quad (5)$$

The specific heat difference, ΔC_p, has been taken as ΔS_m, the entropy of fusion. This assumption holds for a number of glass-forming alloys showing an ordering tendency in the liquid state [17]. This is likely to be the case also for systems solidifying as quasicrystals because it is thought that the icosahedral structure of the solid locally pre-exists in the corresponding liquid [18]. Richards' rule has been applied to estimate the entropy of fusion of Al_6Mn and Al_4Mn as $\Delta S_m = R$ (gas constant), so the enthalpies of fusion are 9.25 and 9.6 kJ mol^{-1}, respectively.

In computing the Al–Mn phase diagram, values of 14.95 and 17.10 kJ mol^{-1} K^{-1} for the entropy of fusion of the above compounds were earlier employed, which are typical of ordered phases [3]. We have also used these values in our computer program and the same qualitative results were obtained as when using lower entropies of fusion. However, the critical cooling rate for avoiding Al_6Mn nucleation is too low in this case (around 10^2 K sec^{-1}) in comparison with experimental practice. This also occurs if the specific heat difference is taken equal to zero in Equation 5, as happens for pure metals. It is also possible that some self-cancelling of errors has occurred in considering the various parameters for our calculation leading to this discrepancy. However, we suggest, as a justification for our choice, that not only the solid but the liquid also could be chemically ordered, implying a low entropy of fusion, as appears to occur for some glass-forming alloys [19]. In order to check this further, we have prepared an Al_3Fe compound which is the only one among all the intermetallic phases present in aluminium-based quasicrystal-forming systems, that melts congruently at 1430 K. Its heat of melting has been estimated from differential thermal analysis traces obtained from alloy samples, after comparison with that of pure copper and silver samples containing about the same number of moles of atoms. The entropy of fusion turns out to be 8.5 ± 1.5 J mol^{-1} K^{-1}.

To estimate ΔG_m we consider the following reaction sequence that occurs in $Al_{80}Mn_{20}$ alloys which are almost single-phase icosahedral

$$\mathrm{I} \rightarrow \Delta H_1 \rightarrow \mathrm{T} \rightarrow \Delta H_1' \rightarrow Al_4Mn \rightarrow \Delta H_2 \rightarrow \mathrm{liq}$$
$$\uparrow \text{———} \Delta H_3 \text{——} \Delta H_4 \text{———} \quad (6)$$

On cooling the liquid we assume that the melting point of I is encountered. Follstaedt and Knapp [20] have very recently shown that the temperature, T_0, at which the free energy of the icosahedral phase equals that of the liquid is 1110 ± 20 K at the Al_6Mn composition, i.e. a few tens of degrees below the extrapolated melting points of the compounds (Fig. 2). On heating, the I-phase transforms at T_t to the T-phase which eventually gives the equilibrium Al_4Mn. The enthalpy balance for Reaction 6 is

$$\Delta H_1 + \Delta H_1' + \Delta H_2 - \Delta H_3 - \Delta H_4 = 0 \quad (7)$$

where $\Delta H_1 = -0.5$ kJ mol^{-1} and $\Delta H_1' = -0.7$ kJ mol^{-1} [15] are the heats of decomposition of the icosahedral and decagonal T-phases, respectively, ΔH_2 is the heat of fusion of λ, and ΔH_3 that of the I-phase. In ΔH_4, the difference in specific heat between liquid and crystal phases is taken into account for the undercooling regime

$$\Delta H_4 = \int_{T_0}^{1153} \Delta C_p \, dT \quad (8)$$

where $\Delta C_p = C_{p,liq} - C_{p,sol} = \Delta S_m$, according to the above approximation, giving $\Delta H_4 = 0.3$ kJ mol^{-1}. The contribution to the enthlapy cycle coming from the specific heat difference may need a further correction because it has been found that the specific heat of the icosahedral phase is 0.8 J mol^{-1} K^{-1} higher than that of equilibrium Al_6Mn [21]. If this were also the case for Al_4Mn, another enthalpy contribution to Equation 7 would come from

$$\Delta H_5 = -\int_{t_t}^{T_0} (C_{p,I} - C_{p,sol}) \, dT = -0.5 \text{ kJ mol}^{-1} \quad (9)$$

Therefore we conclude that ΔH_3, the enthalpy of fusion of the I phase is 9.1 kJ mol^{-1}. From the above discussion, the conclusion is also drawn that ΔH_1, ΔH_4 and ΔH_5 being positive, $\Delta H_3 < \Delta H_2$. On application of Equation 5 to the two solidification paths, this implies a lower ΔG_m for the formation of I than for Al_4Mn (Fig. 3).

From the above discussion we obtain the entropy of fusion of the I-phase as 8.2 J mol^{-1} K^{-1}. For an alloy containing the Al_6CuLi_3 I-phase as the predominant component, the entropy of fusion has been determined to be 7.8 J mol^{-1} K^{-1} [22]. Because the alloy was not exactly single-phase icosahedral, the latter figure should be considered as a lower limit for ΔS_m. However, compared to this finding, our estimate seems reasonable. The free energy difference between λ and the liquid at 1113 K is given approximately by $\Delta G = \Delta S_m$ (1153–1113) = 330 J mol^{-1} which equals the free energy difference between the I- and λ-phases. The entropy difference between I and λ is found to be around 1.4 J mol^{-1} K^{-1} at the melting point of I and, taking into account the specific heat difference between the latter phases, it should become 1 J mol^{-1} K^{-1} at the transformation temperature of I. It is noteworthy that an estimate of the entropy difference between I and Al_6Mn based on a geometrical construction of a Penrose tiling gave $\Delta S = 0.8$ J mol^{-1} K^{-1} [23].

As a check, let us apply the enthalpy cycle (Equation

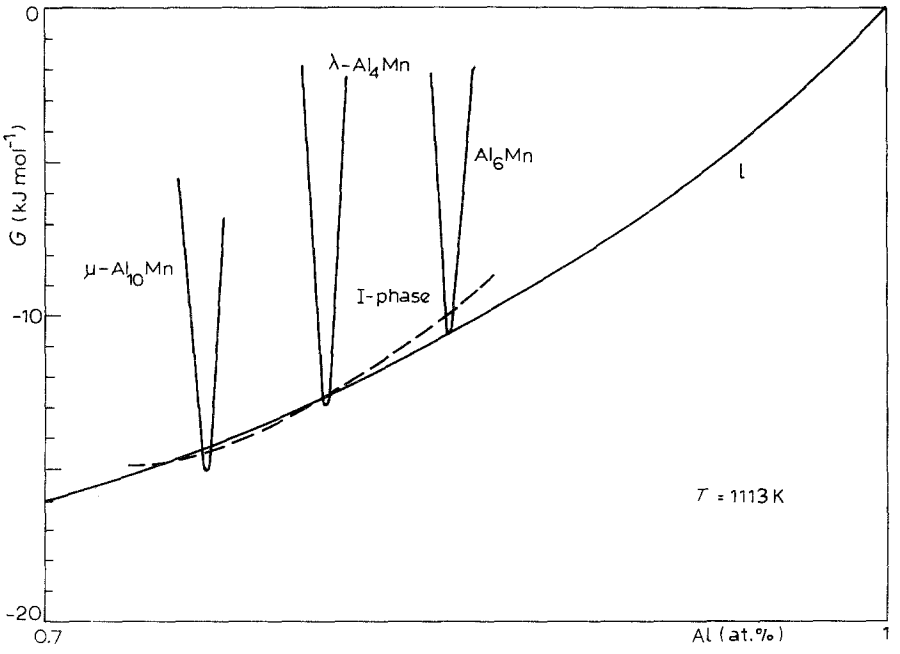

Figure 2 Free energy curves for Al–Mn phases at the melting point of Al_6Mn. The liquid curve is taken from the fitting of experimental data performed in [3]. The curve for the intermetallic compounds and the I-phase are schematic but their position with respect to the liquid is determined according to the discussion in the text.

6) to the transformations occurring in $Al_{86}Mn_{14}$

$$\text{I} + \text{fcc Al(Mn)} \rightarrow \Delta H_1 \rightarrow \text{Al}_6\text{Mn} \rightarrow \Delta H_2 \rightarrow \text{liq}$$
$$\uparrow \qquad\qquad \Delta H_3,\ \Delta H_4,\ \Delta H_5 \qquad\qquad \downarrow \tag{10}$$

The heat of transformation, ΔH_1, is now 1.7 kJ mol^{-1}, T_0 is 1055 K and the melting point of Al_6Mn is 1113 K; so, ΔH_3, the heat of solidification of the liquid into I + fcc Al(Mn) is 7.8 kJ mol^{-1}. The free energy difference between liquid and I-phase, computed as above, is 0.6 kJ mol^{-1} for the Al_6Mn composition at the I melting point. The free energy of the various phases is plotted in Fig. 2 at 1113 K in order to show the driving force for the various solidification paths. The free energy of the liquid is the actual curve optimized from experimental data [3]. The reference points are the pure liquid elements. The curves of the intermetallic compounds are schematic and that of the I-phase is broadened to account for its existence in a composition range and is based on the free energy difference between the phases computed above.

The solid–liquid interfacial tension, γ, has been computed for the undercooling regime by means of the Spaepen equation [24]

$$\gamma = \alpha_m \Delta S_m T/(N_a V^2)^{1/3} \tag{11}$$

where V is the molar volume, N_a the Avogadro constant and α_m a constant, the value of which has been taken as 0.71 as in the case of a number of glass-forming systems [7]. This position is somewhat arbitrary because the above equation was derived for simple solid structures and its extension to complex intermetallic phases can be justified only a posteriori from the results of the computing model. Due to this uncertainty, we have not introduced a further geometrical parameter in ΔG to account for the likely possibility of heterogeneous nucleation of the intermetallics. Further, there have been reports that the interfacial tension between liquid and icosahedral phase should be small as a consequence of the postulated similarity between liquid and solid structures [1, 19]. In the present calculation we have left it as an adjustable parameter in order to check this assumption.

4. Critical cooling rates

The overall transformation kinetics for $Al_{86}Mn_{14}$ alloys is summarized in the TTT curves of Fig. 4. A CCT curve for Al_6Mn is also included which has been obtained by numerical integration of the transformed fractions at each temperature according to the procedure described in [7]. From the endpoint of the CCT curve, the critical cooling rate for the avoidance of Al_6Mn formation from the melt is obtained as 2×10^4 K sec^{-1}. This figure is comparable with previous estimates for quasicrystal formation (10^4 to 10^5) based on the size of icosahedral crystals in atomized droplets [18] and electron-beam scanning experiments [4]. It is worthwhile to remark that once the metastable solid has solidified in a large part of the

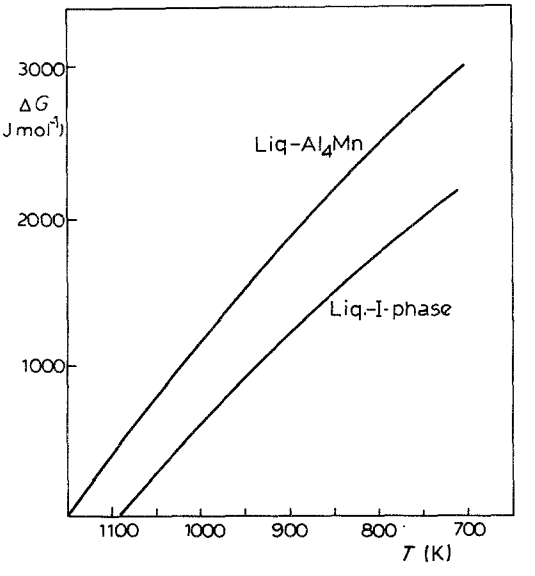

Figure 3 Computed free energy difference between liquid and solid phases in the undercooling regime for $Al_{80}Mn_{20}$.

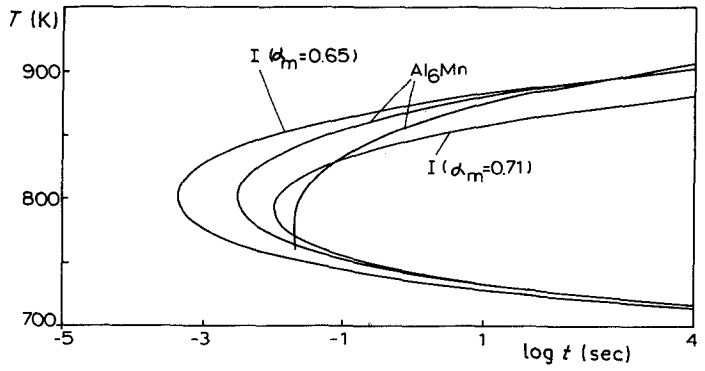

Figure 4 Time–temperature–transformation (TTT) and continuous cooling transformation (CCT) curves for solidification of the phases in $Al_{86}Mn_{14}$.

matrix, the chemical driving force for the formation of the equilibrium phases is substantially reduced. So the above critical cooling rate must be referred only to Al_6Mn solidifying from the melt and not to its possible formation through a solid state reaction by decomposition of the I-phase. However, a cooling rate of this order must be reached to permit the nucleation of I as the first solid.

In the case of heterogeneous nucleation, ΔG^* would be lowered by a quantity depending on the wetting angle between solid and liquid, which is not known. Also the number of atoms involved in the nucleation event would be lowered substantially (from $\sim 10^{28}\,m^{-3}$ to $\sim 10^{19}\,m^{-2}$) with an influence on the overall kinetics opposite to that of ΔG^*. The resulting effect of heterogeneous nucleation would be an increase of the formation rate of the intermetallic compounds. Consideration of the experimental and computed values of the critical cooling rate leads to the supposition that either the effect of heterogeneous nucleation is small or, more acceptably, that the α_m value chosen for Equation 11 (see below) already contains a correction to ΔG^* in the sense expected for heterogeneous nucleation. In any case the following observations will hold. In Fig. 4 the TTT curve for the start of the Al_6Mn crystallization is compared with two possible curves for the icosahedral phase. In the first case (curve a) the same interfacial tension has been used for the two solids. In this event the TTT curve for the I-phase does not protrude out from that of Al_6Mn so it would be impossible to form it on quenching. If the value for the interfacial tension is lowered, the field of solidification of the I-phase becomes substantial at high cooling rates. Curve b in Fig. 4 has been obtained by using a value of 0.65 for α_m in Equation 11. Therefore, we conclude that, within the limits of the present approach, the hypothesis of a low crystal–melt interface energy for icosahedral phases yields confirmation. From the present results, the interfacial energy between I and Al_6Mn is estimated as $0.046\,J\,m^{-2}$ at the melting point of I and $0.027\,J\,m^{-2}$ at the temperature of transformation of the I-phase, 750 K, which compares well with the value of $0.03\,J\,m^{-2}$ obtained from a fit of differential scanning calorimetry (DSC) peaks by means of an Avrami analysis of the transformation [25].

The TTT curves for $Al_{80}Mn_{20}$ are shown in Fig. 5. In addition to Al_4Mn, a curve for the metastable T-phase has been introduced. This phase seems to nucleate and grow epitaxially on I [4] and does not commonly appear in rapidly quenched ribbons at compositions lower than 18% Mn [5]. We have assumed that the I-phase should be present to form T and we have computed from an enthalpy cycle as in Equation 6 that ΔH_m is $9.6\,kJ\,mol^{-1}$ for T. The TTT curve is therefore all internal to that of I and a critical cooling rate of $2 \times 10^6\,K\,sec^{-1}$ is necessary to avoid its nose. This is consistent with the experimental finding that the I-phase can be formed with more difficulty in $Al_{80}Mn_{20}$ than in $Al_{86}Mn_{14}$ [1] and with the experimental TTT curve obtained by quenching three Al–Mn alloys under high pressure [26].

The low interfacial tension together with the reduced value of the free energy difference has an effect on the computed nucleation rate which is considerably higher (Fig. 6). At a cooling rate of 2×10^6 the TTT curve will be entered at 800 K where the homogeneous nucleation rate of I is of the order of $4 \times 10^{16}\,m^{-3}\,sec^{-1}$. It reaches a maximum value of $1 \times 10^{26}\,m^{-3}\,sec^{-1}$ at 775 K and, at the temperature of the nose, 830 K, it is $2 \times 10^{23}\,m^{-3}\,sec^{-1}$. At the same temperature the nucleation frequency for Al_4Mn is $1 \times 10^{16}\,m^{-3}\,sec^{-1}$, several orders of magnitude smaller. We will expect a number of icosahedral particles of $1 \times 10^{18}\,m^{-3}$ in a ribbon [5], which would imply that a homogeneous nucleation rate of 10^{23} may

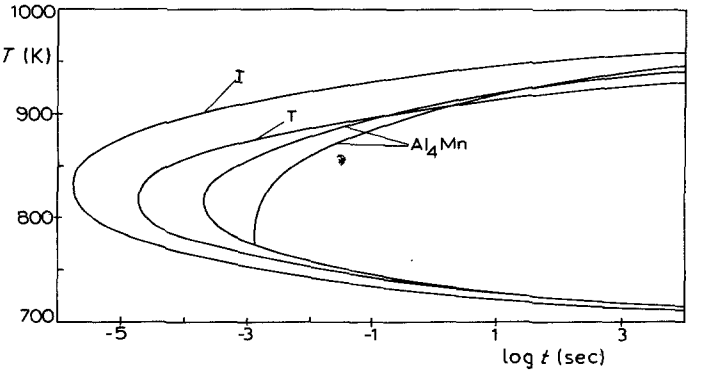

Figure 5 TTT and CCT curves for solidification of the phases in $Al_{80}Mn_{20}$.

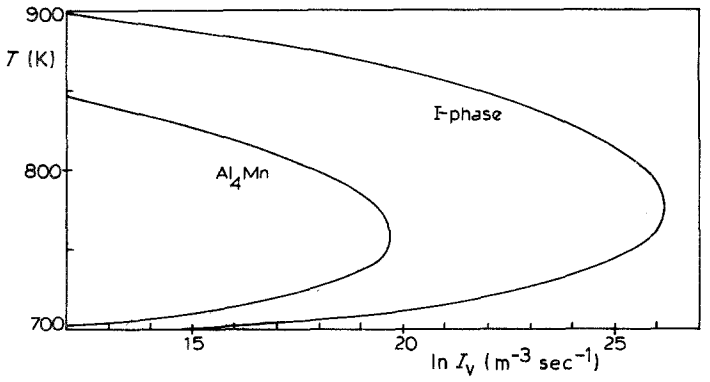

Figure 6 Computed nucleation frequency plotted against temperature for the I-phase and λ-Al_4Mn intermetallic in $Al_{80}Mn_{20}$.

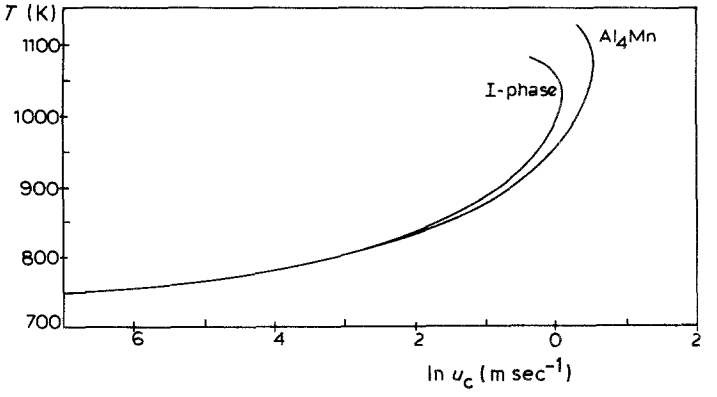

Figure 7 Computed growth rate plotted against temperature for the I-phase and the Al_4Mn intermetallic in $Al_{80}Mn_{20}$.

have been operating for 10^{-5} sec. At a cooling rate of 2×10^6 K sec^{-1} this corresponds to 20 K, which is a correct figure for the width of the solidification field between limiting TTT curves, and to a quench time of the order of a millisecond which is typical of the melt-spinning process. A common dimension of the icosahedral grains in melt-spun ribbons is 1 μm [5, 27], so 1×10^{18} particles per m^3 would fill almost completely the space of the sample.

The present numbers for the nucleation rate would be consistent also with the case of atomized droplets where the highest nucleation rate has been sampled, so 10^{24} particles per cubic meter have been found [18]. The computed growth rate in the temperature range of solidification varies from 7×10^{-2} m sec^{-1} at 880 K to 3×10^{-3} m sec^{-1} at 820 K which on average would lead to micrometre grain dimension in the actual quenching time. At corresponding temperatures the growth rate of Al_4Mn is slightly higher than that of the I-phase as expected from the higher chemical driving force for growth (Fig. 6). The radius of the critical nucleus is 1.3 nm at 880 K and 1.0 nm at 830 K, therefore the nuclei would contain from about 800 to 400 atoms.

The fast nucleation of the quasicrystalline phases prevents glass formation by rapidly quenching the melt in these systems. A chemical modification of the alloy by addition of silicon progressively shifts the TTT curves to higher times making formation of the I-phase easier at first, at about 5 at % Si, and finally glass formation possible.

Acknowledgement

This work is supported by ENEA-Rome, under contract no. 3405 Università di Torino, ENEA.

References

1. L. A. BENDERSKY and R. J. SCHAEFER, *Physica* **140A** (1986) 298.
2. Papers presented at the International Workshop on Aperiodic Crystals, Les Houches, *J. de Phys.* **47–C3** (1986) 351.
3. J. L. MURRAY, A. J. McALISTER, R. J. SCHAEFER, L. A. BENDERSKY, F. S. BIANCANIELLO and D. L. MOFFAT, *Met. Trans. A* **18A** (1987) 385.
4. R. J. SCHAEFER, L. A. BENDERSKY and F. S. BIANCANIELLO, *J. de Phys. Coll.* **C3** 47 (1986) 311.
5. R. J. SCHAEFER, I. A. BENDERSKY, D. SHECHTMAN, W. J. BOETTINGER and F. S. BIANCANIELLO, *Met. Trans. A* **17A** (1986) 2117.
6. R. J. SCHAEFER, *Scripta Metall.* **20** (1986) 1187.
7. L. BATTEZZATI, C. ANTONIONE and G. RIONTINO, *J. Non-Cryst. Solids* **89** (1987) 114.
8. R. URBAN, N. MOSER and H. KRONMÜLLER, *Phys. Status Solidi (a)* **91** (1985) 411.
9. H. S. CHEN and C. H. CHEN, *Phys. Rev. B* **33** (1986) 668.
10. R. A. DUNLAP and K. DINI, *J. Mater. Res.* **1** (1986) 415.
11. S. J. POON, A. J. DREHMAN and K. R. LAWLESS, *Phys. Rev. Lett.* **55** (1985) 2324.
12. J. W. CHRISTIAN, "The Theory of Transformations in Metals and Alloys" (Pergamon, Oxford, 1975).
13. E. S. LEVIN, M. S. PETRUSHEVSKII, P. V. GEL'D and G. D. AYUSHINA, *Russ. J. Phys. Chem.* **46** (1972) 1263.
14. *Idem, ibid.* **46** (1972) 807.
15. K. KIMURA, T. HASHIMOTO, K. SUZUKI, K. NAGAYAMA, H. INO and S. TAKEUCHI, *J. Phys. Soc. Jpn* **55** (1986) 536.
16. R. A. DUNLAP and K. DINI, *Can. J. Phys.* **63** (1985) 1267.
17. L. BATTEZZATI and M. BARICCO, *Phil. Mag. A* **56** (1987) 139–146.
18. L. A. BENDERSKY and S. D. RIDDER, *J. Mater. Res.* **1** (1986) 405–414.
19. N. SAUNDERS, *CALPHAD* **9** (1985) 297.
20. D. M. FOLLSTAEDT and J. A. KNAPP, *Mater. Sci. Engng* **99** (1988) 367.

21. H. S. CHEN, C. H. CHEN, A. INOUE and J. T. KRAUSE, *Phys. Rev. B* **32** (1985) 1940.
22. K. N. RAO and J. A. SEKHAR, *Scripta Metall.* **21** (1987) 13.
23. L. C. CHEN and F. SPAEPEN, *Mater. Sci. Engng.* **99** (1988) 339.
24. F. SPAEPEN and D. TURNBULL, in "RQM II", edited by N.J. Grant and B.C. Giessen (MIT Press, Cambridge, Mass., 1976) pp. 205–230.
25. K. F. KELTON and J. C. HOLZER, *Mater. Sci. Engng* **99** (1988) 389.
26. G. S. REDDY, J. A. SEKHAR and P. V. RAO, *Scripta Metall.* **21** (1987) 13.
27. L. BATTEZZATI, C. ANTONIONE and F. MARINO, *Scripta Metall.* **22** (1988) 623.

Received 29 February
and accepted 10 November 1988